

AD-A034 680

PRATT AND WHITNEY AIRCRAFT WEST PALM BEACH FLA FLOR--ETC F/G 20/5  
CYLINDRICAL POLISHING TECHNOLOGY DEVELOPMENT PROGRAM, (U)  
JUL 75 T B MILAM  
PWA-FR-7108

N00014-74-C-0338

NL

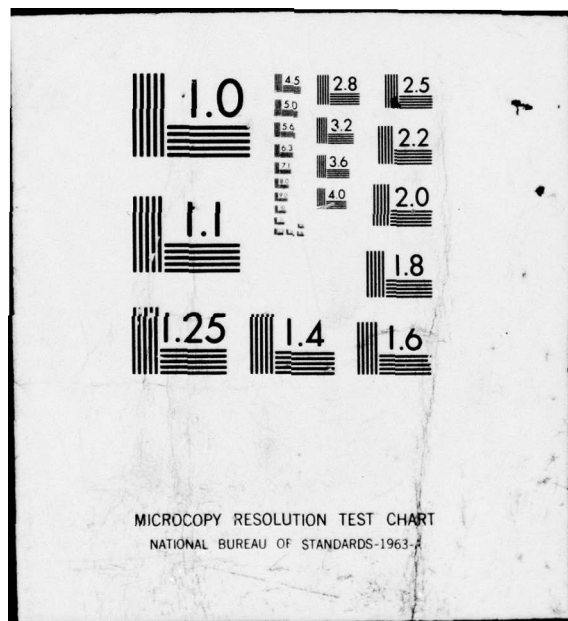
UNCLASSIFIED

| OF |  
AD  
A034680

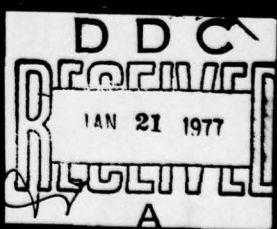


END

DATE  
FILMED  
2-77



ADA 034680



## UNCLASSIFIED

SECURITY CLASSIFICATION OF THIS PAGE (When Data Entered)

REPORT DOCUMENTATION PAGE			READ INSTRUCTIONS BEFORE COMPLETING FORM
1. REPORT NUMBER	2. GOVT ACCESSION NO.	3. RECIPIENT'S CATALOG NUMBER	
4. TITLE (and Subtitle) Cylindrical Polishing Technology Development Program.		5. TYPE OF REPORT & PERIOD COVERED Final Report. 3 June 1974 - 31 July 1975	
6. PERFORMING ORG. REPORT NUMBER PWA		7. CONTRACT OR GRANT NUMBER(s) N00014-74-C-0338 NEW	
8. PERFORMING ORGANIZATION NAME AND ADDRESS Pratt & Whitney Aircraft Division United Technologies Corporation Florida Research and Development Center Box 2691 West Palm Beach, Florida 33402		9. PROGRAM ELEMENT, PROJECT, TASK AREA & WORK UNIT NUMBERS	
10. CONTROLLING OFFICE NAME AND ADDRESS Office of Naval Research Department of the Navy Arlington, Virginia 22217		11. REPORT DATE 31 July 1975	
12. MONITORING AGENCY NAME & ADDRESS (if different from Controlling Office) Director Naval Research Laboratory (Code 5540) 4555 Overlook Avenue, South West Washington, D. C. 20375		13. NUMBER OF PAGES 25	
14. DISTRIBUTION STATEMENT (of this Report) Reproduction in whole or in part is permitted for any purpose by the United States Government 1227p.		15. SECURITY CLASS. (of this report) Unclassified	
16. DISTRIBUTION STATEMENT (of the abstract entered in Block 20, if different from Report)		15a. DECLASSIFICATION/DOWNGRADING SCHEDULE	
17. DISTRIBUTION STATEMENT (of the abstract entered in Block 20, if different from Report)		DISTRIBUTION STATEMENT A Approved for public release; Distribution Unlimited	
18. SUPPLEMENTARY NOTES		D D C RECORDED JAN 21 1977 A	
19. KEY WORDS (Continue on reverse side if necessary and identify by block number) Optical Polishing Metal Optics Cylindrical Mirrors Laser Mirrors			
20. ABSTRACT (Continue on reverse side if necessary and identify by block number) Cylindrical optical figures are needed for high energy laser (HEL) mirrors constructed of molybdenum material. The subject program determined the state-of-the-art for polishing molybdenum to cylindrical optical figures and advanced the technology within funding limits. * * * * * micrometer Cylindrical optical figures of $\lambda/2$ ( $\lambda \approx 0.5 \mu\text{m}$ ) quality were determined to be state-of-the-art at PWA-FRDC during the early stages of the program, but this quality was subsequently improved to $\lambda/4$ . →			

UNCLASSIFIED

SECURITY CLASSIFICATION OF THIS PAGE(When Data Entered)

It proved to be impractical, if not impossible, to establish quantitative effects of the process variables, or to relate the process to spherical polishing technology.

Of the several inspection techniques investigated, the glass test plate/monochromatic light interferometer and the noncontact slit interferometer (described in the text) appeared to be the best available techniques to ensure figure quality specifications are met.

UNCLASSIFIED

SECURITY CLASSIFICATION OF THIS PAGE(When Data Entered)

## FOREWORD

This report contains the results of a cylindrical mirror polishing program performed under contract N00014-74-C-0338 sponsored by the Office of Naval Research. The program was performed by Pratt & Whitney Aircraft at the Florida Research and Development Center, and was experimental in nature as opposed to analytical.

## CONTENTS

SECTION	PAGE
ILLUSTRATIONS .....	4
I INTRODUCTION .....	5
II EXPERIMENTAL POLISHING PROGRAM .....	7
III INSPECTION TECHNOLOGY PROGRAM .....	16
IV CONCLUSIONS AND RECOMMENDATIONS .....	25

*Letter on file*

ACCESSION NO.	
NTIS	White Section
DOC	Buff Section
UNARMED/ARMED	
JUDGMENT	
BY	
DISTRIBUTION/AVAILABILITY CODES	
B&W	AVAIL. 200/OF SPECIAL
A	

## ILLUSTRATIONS

FIGURE	PAGE
1 Cylindrical Mirror Polishing Diagram.....	5
2 Cast Iron Lap .....	7
3 Wax Lap.....	8
4 Strausbaugh Model 6AK-2 Cylindrical Polishing Machine .....	9
5 Schematic of Cylindrical Polishing Machine .....	10
6 Polishing Action for Several Axial-to-Radial Stroke Ratios .....	10
7 Generation of Rough Cylindrical Surfaces.....	12
8 Bucone Machine.....	14
9 Cylindrical Polishing Machine Motions .....	15
10 Electronic Sagital Micrometer .....	17
11 Optical Test Plate Inspection .....	17
12 Inspection Planes.....	18
13 ZYGO Interferometer Line Fringe Pattern .....	19
14 Foucault Test Setup .....	20
15 Foucault Knife Edge Test .....	20
16 Foucaultgram of a Cylindrical Surface .....	21
17 Slit Interferogram .....	22

## SECTION I

### INTRODUCTION

An experimental polishing program was performed to identify and to advance the state-of-the-art for manufacturing cylindrically figured optical surfaces of the type needed for high energy laser mirrors. Optical inspection techniques for cylindricals were also investigated.

Polishing procedures for molybdenum and for glass samples of the type illustrated in Figure 1 were studied. Molybdenum was selected because it is at present the optimum high energy laser mirror material, and glass because a glass test plate is needed to evaluate the molybdenum surface during polishing.

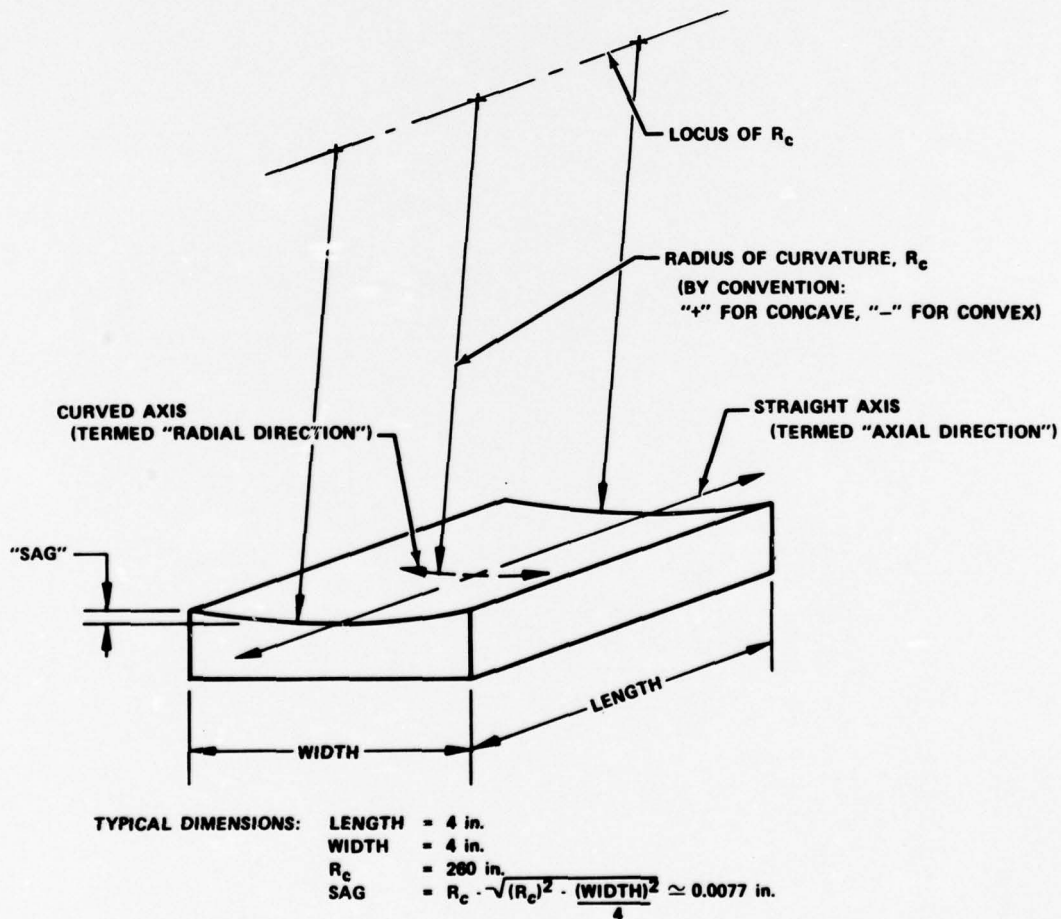


Figure 1. Cylindrical Mirror Polishing Diagram

FD 91286

**Finishing technology for optical quality spherical surfaces has been well developed (and documented to some extent); finishing technology for nonaxisymmetric surfaces such as the cylindrical is virtually nonexistent.**

**During the program two types of cylindrical polishing machines were used and several types of surface inspection techniques were investigated. These experiments are discussed herein.**

## SECTION II

### EXPERIMENTAL POLISHING PROGRAM

#### GENERAL

The "conventional" manufacture of optically precise surfaces involves a process of gradual material removal or displacement at the optical surface and frequent checks to assess the progress of the process. Optically smooth surfaces are achieved by lapping with progressively smaller abrasives as the deeper scratches and digs from previous abrasives are erased. Hard laps such as cast iron (Figure 2) or glass are used initially where figure corrections (i. e., overall radius of curvature) are required. Once the near correct figure quality is achieved, soft laps such as wax (Figure 3) or felt pad are used with still smaller abrasives to correct small scale surface irregularities and to improve the micro-finish of the surface. Very little if any overall figure change occurs after progressing to the soft lap because of the small abrasives used and because the soft lap tends to conform to the surface configuration of the work piece. Abrasive sizes range from  $40 \mu\text{m}$  down to submicron sizes depending on the type of materials involved. The process is often designated "free abrasive grinding" when a hard lap is used, and "polishing" when a soft lap is used.

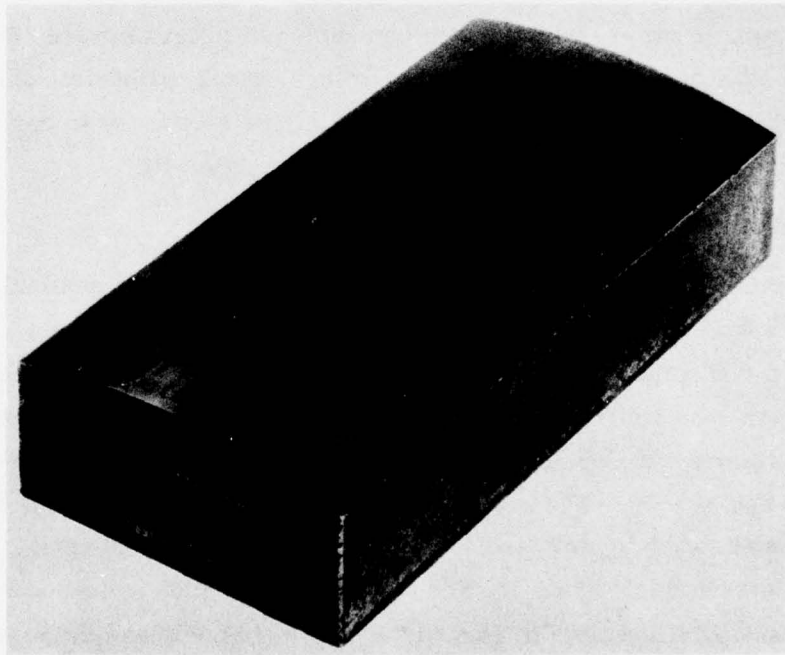


Figure 2. Cast Iron Lap

FE 124132

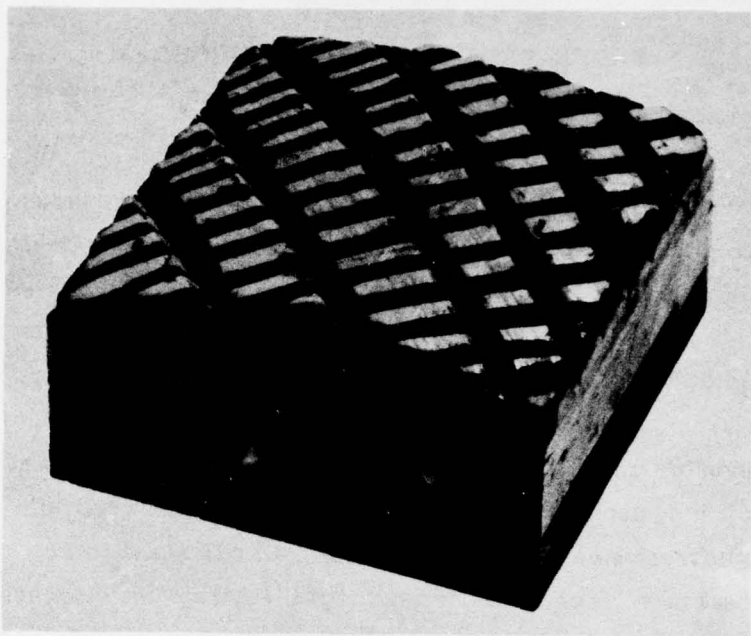


Figure 3. Wax Lap

FE 124133

A limit to the surface figure quality achievable is the ability to readily inspect and locate errors in the optical surface. In theory, once an error is detected and located, adequate machine and process variables can be set to correct the error. Primary goals of this experimental program were (1) to establish practical means of detecting and locating errors during cylindrical polishing, and (2) to determine the machine and process variations necessary to correct the errors. Optical inspection of cylindricals is discussed in Section III.

#### STRAUSBAUGH MACHINE MODEL 6AK-2 RESULTS

The experimental polishing effort was initiated using an available Strausbaugh Model 6AK-2 cylindrical polishing machine shown in Figure 4. This machine has two spindles, each capable of working cylindrical surfaces up to about 17.8 cm x 38 cm (7 in. x 15 in.). The spindles can be oscillated (radial motion) or rotated 360 deg about their axes at a continuously variable rate between 12 and 80 cpm. The overarms are driven axially and parallel to the spindle axes at rates continuously variable between 10 and 120 cpm. The machine action is illustrated in Figure 5. The type relative motion produced between lap and work piece is illustrated in Figure 6. The work piece and the tool can be mounted in either position; however, it was observed with long radii parts that best results were obtained with the concave element mounted on the overarm.

The initial work piece used during the experimental effort was a 5 in. x 5 in. glass substrate which had been previously finished flat on a spherical polishing machine. The purpose of this initial effort was to establish the basic cause-effect relationships of the cylindrical polishing process variables. Changes in the flat surface figure could readily be detected using an available flat test plate or using a ZYGO interferometer.

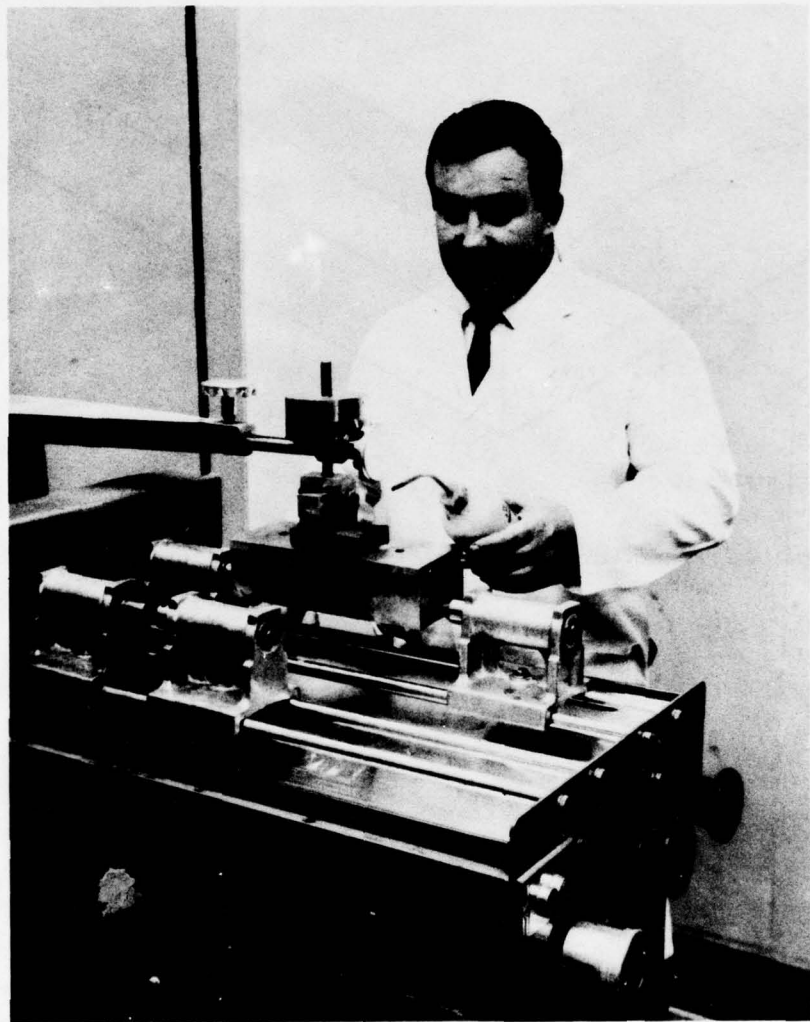


Figure 4. Strausbaugh Model 6AK-2 Cylindrical Polishing Machine

FE 124131

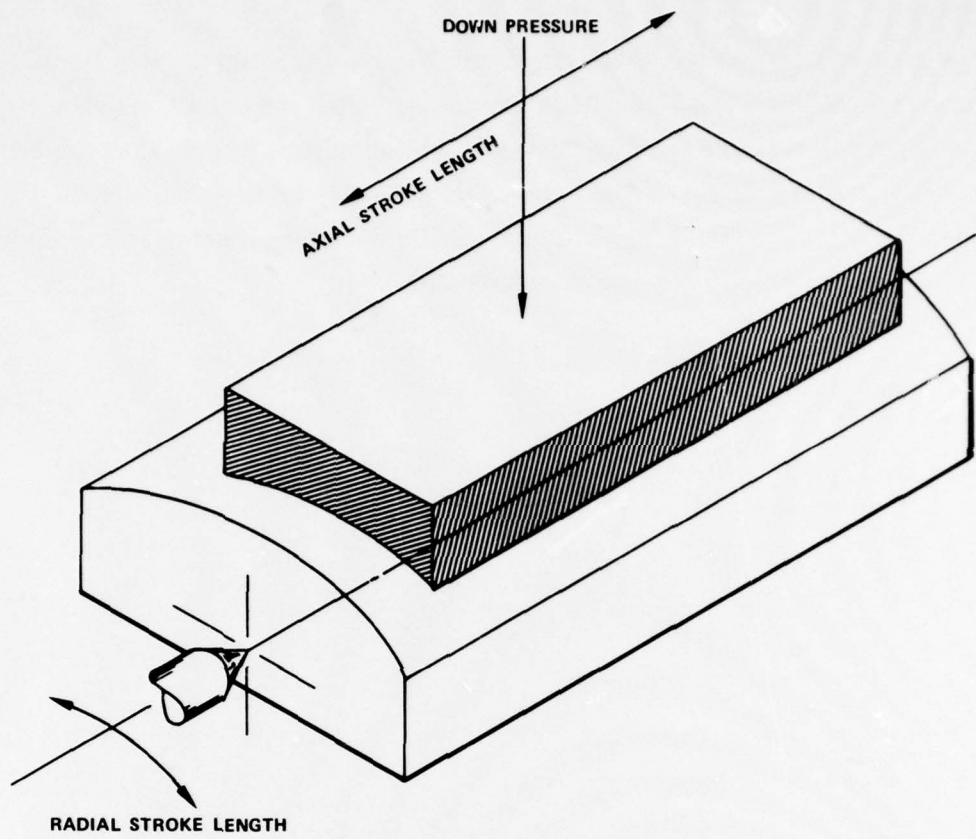


Figure 5. Schematic of Cylindrical Polishing Machine FD 91287

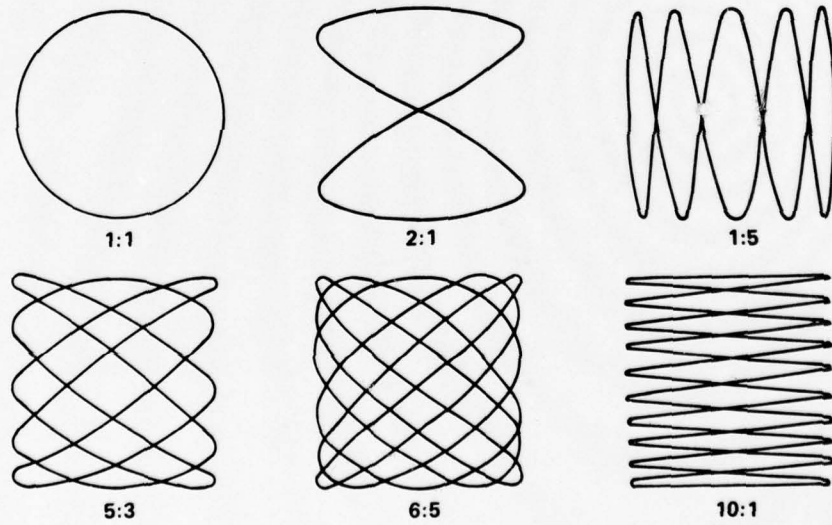


Figure 6. Polishing Action for Several Axial-to-Radial Stroke Ratios FD 84294

It was observed during the initial experimental effort that figure changes in the cylindrical optical surface occurred at a much slower rate than occurred during spherical surface polishing. This was not unexpected because the allowable relative velocity between lap and work piece proved to be much slower on the cylindrical polishing machine than on an axisymmetric machine. It was also observed that the flat surface could be maintained and controlled, suggesting that manufacture of very long radii cylindrical surfaces would be possible. Surface irregularities which were attributed to machine drive train backlash were imparted into the work piece; an irregular drive motion could be sensed by touching the overarm. The magnitude of the irregularity was about  $\lambda/4$  ( $\sim 5 \times 10^{-6}$  in.) and appeared as two linear streaks lying along the length of the sample near each outside edge of the aperture.

Machine parameters were recorded during the polishing but no conclusive relationships could be established because of the large number of interacting process variables; one was the surface figure of the lap which is believed to be responsible for large inconsistencies in results. Laps tend to assume the shape of the work piece and vice versa. Identical changes of variables from time to time, therefore, did not give repeatable results. Some of the process variables are listed in Table 1 to illustrate the complexity encountered when trying to characterize the cylindrical polishing process. As a consequence, optical polishing continues to be a process of trial and error with short cycles and frequent surface figure checks; it is highly dependent on good judgment by the operator in setting the process variables from cycle to cycle.

During an experimental effort to produce a 260 in. radius of curvature cylindrical glass work piece, it was observed that (1) faceted or grooved laps are required to prevent starving of fresh abrasive from the center of the lap, and (2) shape control in the length or axial direction was more difficult than in the width (or radial) direction.

The long radii work pieces and laps were prepared using conventional grinding techniques as illustrated in Figure 7. A cupped grinding wheel, properly tilted with respect to the axial translation of the work piece, produced a surface approaching the desired radius of curvature cylindrical surface. The ground surface is slightly elliptical and must be corrected during the initial stages of "free abrasive grinding" on the cylindrical polishing machine.

TABLE 1. SOME CYLINDRICAL POLISHING VARIABLES

<b>I. GENERAL</b>		<b>IV. LAP PARAMETERS</b>	
A.	Date/Time	A.	Material
B.	Operator	B.	Geometry
C.	Ambient Temperature	1.	Length/Width/Thickness
D.	Cycle Time	2.	Facets
<b>II. MACHINE PARAMETERS</b>		a.	Type
A.	Radial Stroke Speed	b.	Size
B.	Radial Stroke Length	<b>V. WORK PIECE PARAMETERS</b>	
C.	Axial Stroke Speed	A.	Material
D.	Axial Stroke Length	B.	Radius of Curvature
E.	Overarm Load	<b>VI. CYCLE EFFECTS</b>	
F.	Part-to-Lap Position	A.	Work Piece
<b>III. SLURRY PARAMETERS</b>		1.	Surface Finish (rms, Scratch and Dig)
A.	Abrasive	2.	Radius of Curvature
1.	Material	3.	Axial Figure
2.	Size	<b>B.</b>	Lap
3.	Concentration	1.	Surface Finish (rms, Scratch and Dig)
<b>B.</b>	Carrier	2.	Radius of Curvature
1.	Material (Base)	3.	Axial Figure
2.	Additives	<b>C.</b>	
3.	Ph	<b>Rate of Application</b>	
4.	Viscosity		

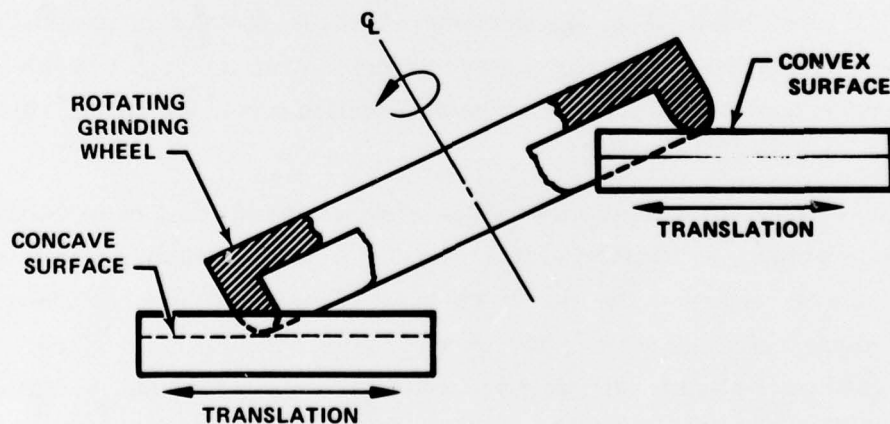


Figure 7. Generation of Rough Cylindrical Surfaces FD 84291

During experimental polishing of molybdenum, performed on the Strausbaugh machine, the material removal rate was observed to be about 25% as fast as for spherical polishing. A circular (round) aperture resulted in curvature in the flat length direction which could not be prevented by various machine settings. A relief ground around a rectangular polishing area in the surface so that a rectangular aperture was presented for polishing subsequently allowed control and correction of the axial curvature. Effort on this sample resulted in a  $\lambda/2$  ( $\sim 10 \times 10^{-6}$  in.) figure quality. A subsequent 152 in.  $R_c$  concave molybdenum surface also resulted in similar quality.

In summary, the experimental effort with the Strausbaugh machine indicated that:

1. Rectangular apertures provided for better figure control
2. Larger laps provided for better overall figure control (i.e., maximum overlap preferred)
3. Smaller laps were required for local figure error (irregularity) corrections
4. Material removal (or displacement) rate was slow due to (1) limited lap load (before chatter occurred), (2) limited stroke speed (before chatter occurred), and (3) the initial starting configurations were generated as an elliptical surface leaving excessive material to be removed during the "free abrasive grinding" cycles
5. The Strausbaugh 6AK-2 design was based on polishing complete cylinders, and excessive backlash occurred when the load direction on the machine drive train was reversed, as required during long radii polishing.

#### BUCONA MACHINE MODEL GP 1212C RESULTS

Because of the need for a machine better suited for long radii cylindrical polishing, 24 vendor sources were contacted. Only two sources offered production (as opposed to custom made) machines with as great as 12 in. aperture size capacity. The Bucone Corporation Model GP 1212C had the highest advertised

quality capability and was selected for procurement. After receipt of this machine (Figure 8), it was fitted with special tooling to allow mounting of laps and work pieces that were geometrically sized to be similar to anticipated mirror geometries. In the Bucone machine, the lower mount is translated linearly, and at independently variable rates, in X and Y directions while the overarm mount is allowed to "float" in the Z axis. A comparison between the actions of the Strausbaugh and Bucone machines is illustrated in Figure 9.

When the Bucone long radii cylindrical polishing machine became available, the experimental polishing program was continued using this equipment. The initial experimental effort was again performed using a prefinished flat glass work piece, but insufficient fixturing (subsequently corrected) resulted in the destruction of the glass work piece. A systematic record of the machine settings and variables was studied, but again no conclusive relationships could be drawn from the recorded data. However, during recent experimental efforts, a figure quality in the latest molybdenum sample (a 200 in. concave sample) of  $\lambda/4$  ( $\sim 5 \times 10^{-6}$  in.) and a surface finish better than 80  $\text{\AA}$  rms have been demonstrated.

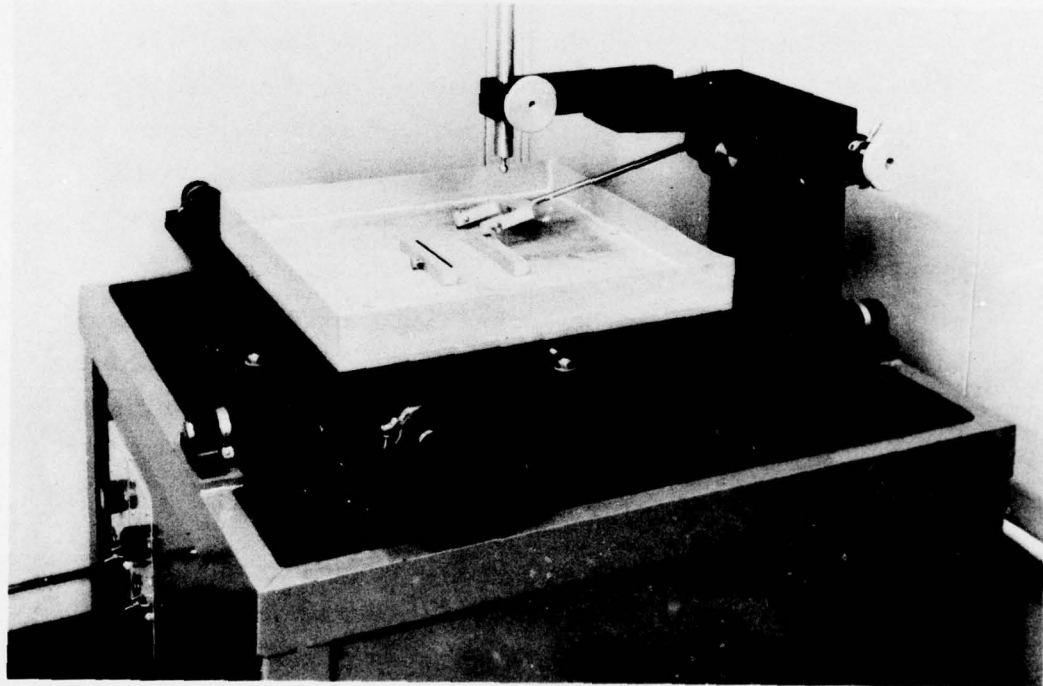


Figure 8. Bucone Machine

FC 31262A

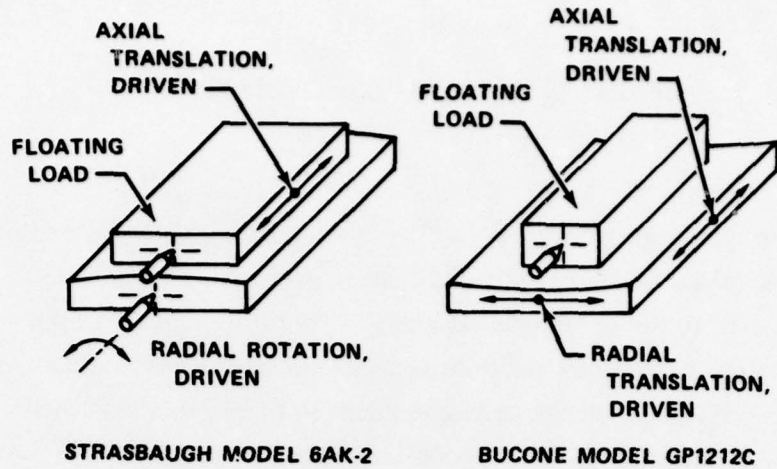


Figure 9. Cylindrical Polishing Machine Motions

FD 84296

## SECTION III

### INSPECTION TECHNOLOGY PROGRAM

#### GENERAL

Greatest gains in cylindrical surface polishing capabilities can be realized through the development of cylindrical surface inspection techniques. The ability to determine the configuration and quality of the optical surface allows the determination of process variable settings for error corrections. The optical inspection of cylindrical surfaces is compounded by the fact that the work piece, if removed from the machine for inspection, must be remounted in the precise orientation as it was originally. For spherical polishing this is not required because of the symmetrical characteristic of spheres. As a result, inspection of cylindricals should be performed without dismounting the workpiece.

To produce high quality optical surfaces, it is essential that the component be inspected regularly and frequently during polishing. "Contact" methods are employed during coarse "free abrasive grinding" and up until the very final stages of polishing. The electronic micrometer (Figure 10) is used effectively before a reflective surface is achieved. The more accurate and easier to use test plate/monochromatic light interferometric technique (Figure 11) can be used after a reasonably reflective surface has been achieved. The problem with the latter technique is that no source for sufficiently accurate cylindrical test plates has been found for a timely and reasonably priced delivery, whereas spherical test plates can generally be procured within 4 weeks and have figure qualities equal to or better than  $1/20$  visual wavelength ( $\lambda_{vis}$ ).

#### NONCONTACT INSPECTION TECHNIQUES

The inspection problem is basically one of achieving a sufficiently precise diagnostic beam waveform. That is, optical surfaces can be inspected to only about  $1/10$  that of the quality of the projected beam. If a lens (or test plate) is  $1/10\lambda$  quality, then the surface under inspection can be quoted to be only  $1/5\lambda$  quality when it appears to be a perfect match to the diagnostic beam (or test plate).

Noncontact inspection techniques have not been developed specifically for cylindrical polishing and, therefore, were an important part of this program. Those studied are discussed below.

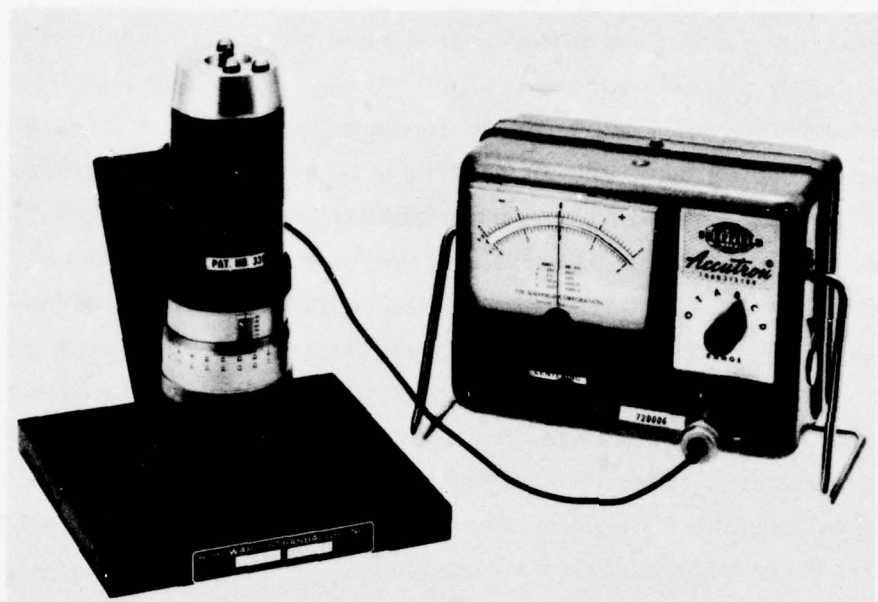


Figure 10. Electronic Sagital Micrometer

FAE 124140

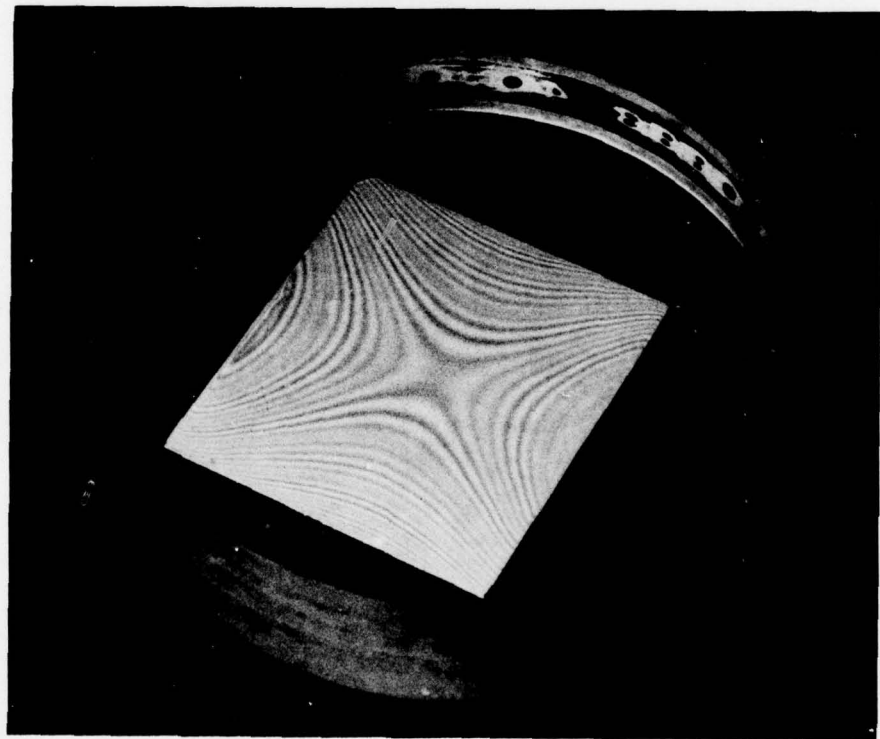


Figure 11. Optical Test Plate Inspection

FAE 124139

## ZYGO Interferometer

A possible approach to achieve a noncontact inspection technique was to procure a highly precise cylindrical lens for the existing ZYGO interferometer. This interferometer is a commercially available item which projects a coherent and collimated object beam onto the surface to be inspected. The reflected beam is aligned and combined with a reference beam (internal to the device) so that a series of fringes appears on the screen of the device. The distortion of the fringes represents the distortion of the reflected beam as a result of imperfection in the optical surface under test. By placing a cylindrical lens in the path of the projected beam, inspection of cylindrical surfaces should be possible. The drawback of this scheme was the unavailability of a sufficiently precise cylindrical lens at a reasonable cost (quoted cost and delivery of such a lens proved to be prohibitive - eight months to a year). Also, several lenses would be required to cover a range of radii of curvature.

The ZYGO interferometer was used, however, to inspect select lines along the optical surface as illustrated in Figure 12. Flat and spherical optical elements are used, and fringe patterns like those shown in Figure 13 result. Such fringe patterns can be analyzed to establish the quality of a cylindrical surface along a specific line.

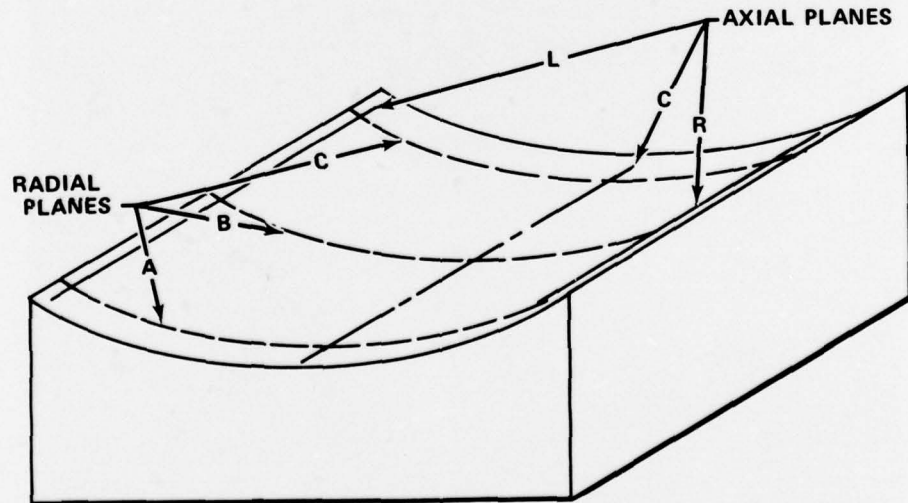


Figure 12. Inspection Planes

FD 67371

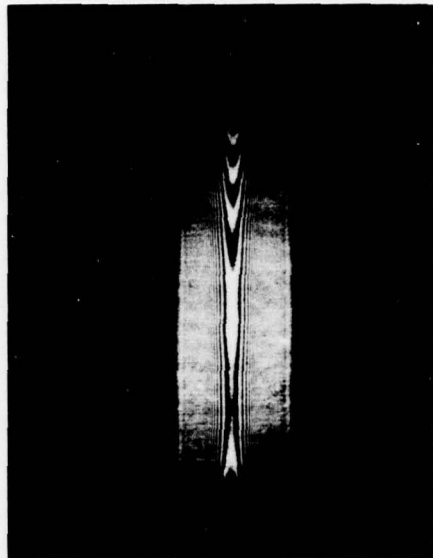
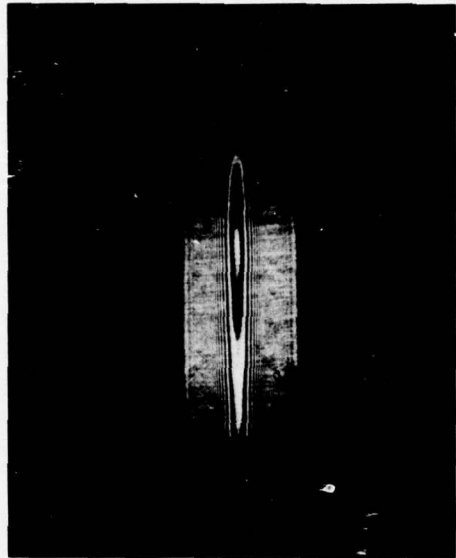


Figure 13. ZYGO Interferometer Line Fringe Pattern

FC 31264

#### Foucault Knife Edge Test

A non-contact type inspection technique used during the program was the Foucault knife edge optical test shown in Figure 14 and schematically in Figure 15. The mirror is positioned with its cylindrical axis in a vertical direction and is illuminated by a light source placed, in effect, at the center of curvature for the mirror. A beam splitter is used to allow the light source to be placed off-axis so that it does not interfere with the projected image of the mirror surface. The image of the mirror surface is projected onto a screen after being partially obstructed at the focal point by a precision knife edge. Irregularities in the mirror surface cause the respective light rays to pass the focal point slightly off-axis. By blocking these light rays with the knife edge, a dark area appears on the screen corresponding to the defect in the mirror. An example of a Foucault test image is shown in Figure 16 (sometimes called a Foucaultgram).

The Foucault test provides a quick qualitative evaluation of the cylindrical optical surface, but a quantitative interpretation, although possible, is tedious and time consuming. Accurate geometrical dimensions of the test setup are required. The magnitude of surface error is also dependent on the knife edge displacement required to produce localized shadows.



Figure 14. Foucault Test Setup

FAE 124137

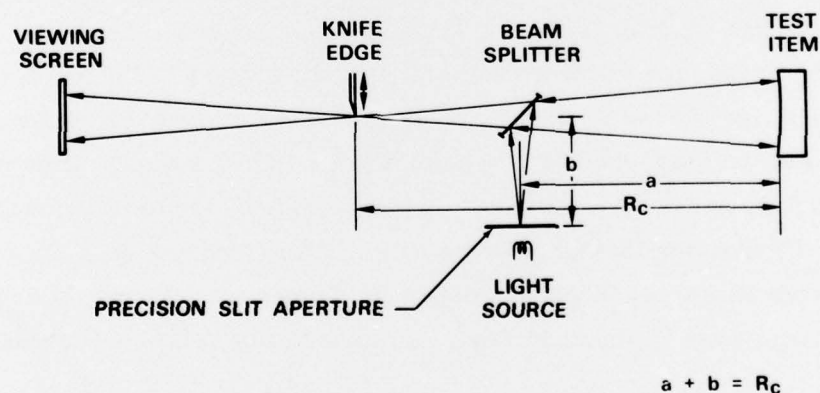


Figure 15. Foucault Knife Edge Test

FD 84297

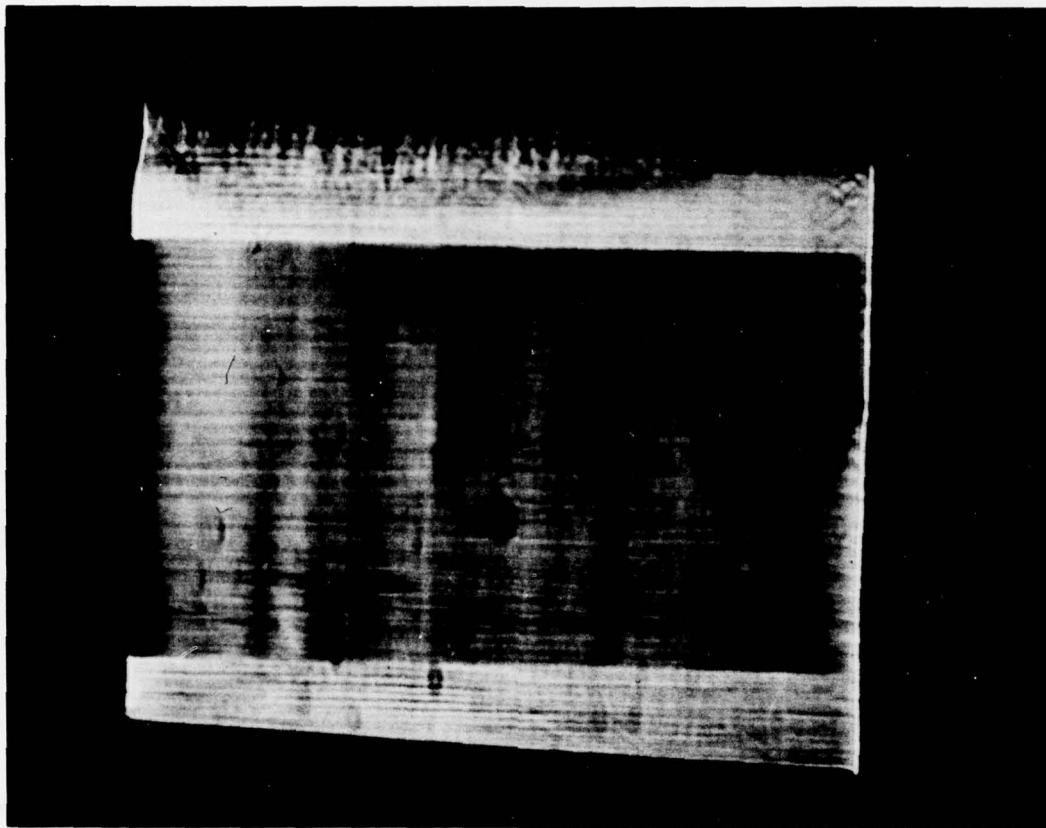


Figure 16. Foucaultgram of a Cylindrical Surface

FE 124141

#### Slit Interferometer

One of the most straightforward methods of assessing the quality of an optical surface is to reflect a coherent beam off the surface and measure the induced phase variation interferometrically. Self-contained interferometric devices are available commercially (such as the ZYGO interferometer) for analyzing flat and spherical mirrors. The accuracy limit of such devices is defined by the quality of the internal optics. Accuracies on the order of  $\lambda/10$  (visible) are readily available.

The use of cylindrical optics is often limited to special applications such as chemical lasers. As a result, the polishing and quality assessment techniques for cylindrical surfaces are not as well developed as for spherical or flat mirrors. High quality cylindrical lenses and mirrors are not readily available.

An assessment of the surface of a concave cylindrical mirror can be made with a slit interferometer which does not use cylindrical optics. Figure 17 is a sketch of a typical slit interferometer system. This type system was verified experimentally during the program. A simple beam splitting scheme is used to separate and then recombine a reference and an object beam and to adjust the relative power levels to maximize fringe contrast. The object beam is made incident on a precision slit. The cylindrical test surface is placed such that the focal line lies within the precision slit. Light diffracting from the slit exhibits a cylindrical phase front which is then collimated by the test piece. Imperfections in the test mirror surface will result in a nonuniform reflected phase front and are defined graphically when the object and reference beams recombine.

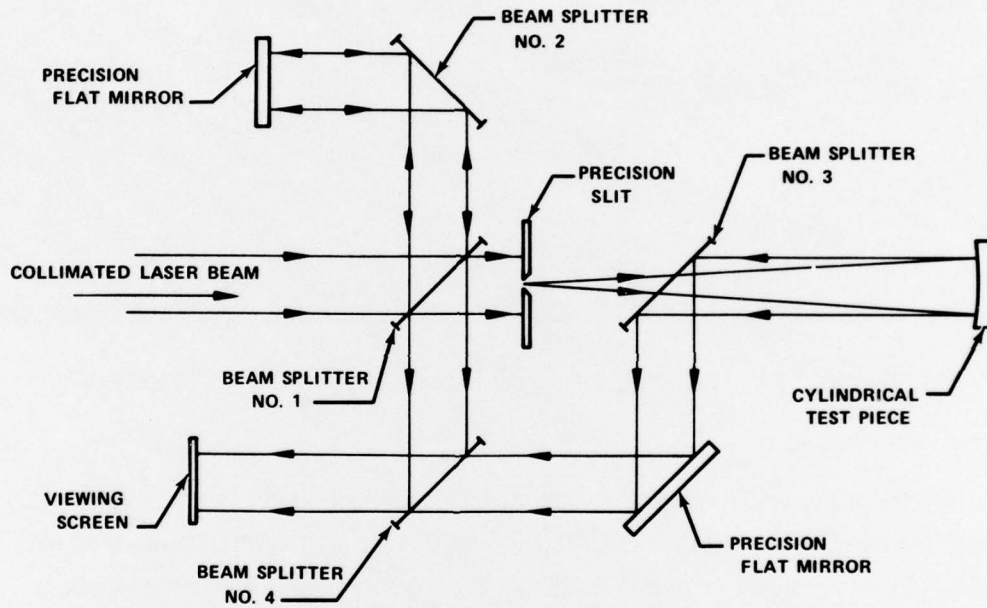


Figure 17. Slit Interferogram

FD 91288

Diffracted light from a slit exhibits a cylindrical phase front only over a limited range, roughly between the Rayleigh range of the slit width and the Rayleigh range of the slit length. The Rayleigh range is defined as the range at which a beam of diameter  $D$  has diffracted to  $2D$ , and

$$\text{Rayleigh range} = \frac{\pi D^2}{4\lambda} \quad (1)$$

The complex amplitude (intensity and phase) exhibited in the near field of a slit aperture is defined by the Fresnel-Kirchhoff equation

$$U_P = \frac{-ik}{4\pi} \int \int_A \frac{U_A e^{i(kr - \omega t)}}{r} \left[ \cos(\hat{n} \cdot \vec{r}) + 1 \right] dA \quad (2)$$

Where  $U_P$  is the complex amplitude at a point  $P$   
 $k$  is the wave number ( $\equiv 2\pi/\text{wavelength, } \lambda$ )  
 $A$  is the aperture area  
 $U_A$  is the complex amplitude incident on the aperture  
 $\vec{r}$  is the vector from a point in the aperture to  $P$   
 $\hat{n}$  is a unit vector normal to the aperture plane  
 $\omega$  is the frequency of light  
and  $t$  is time.

This equation can be evaluated in terms of the Fresnel integrals

$$C(w) = \int_0^w \cos \frac{\pi x^2}{2} dx; \quad S(w) = \int_0^w \sin \frac{\pi x^2}{2} dx$$

as follows:

$$U_P = B \left[ C(u) + iS(u) \right] \frac{u_2}{u_1} \left[ C(v) + iS(v) \right] \frac{v_2}{v_1} \quad (3)$$

where  $u_1$ ,  $u_2$ ,  $v_1$ , and  $v_2$  define the slit edges and  $B$  includes all the constant factors.

The constraints on selection of slit dimensions are general in nature. The slit length should be the full width of the reference beam to provide as near uniform illumination of the test piece as possible. The power incident on the test optic varies roughly as the square of the slit width, providing some control over the absolute intensity level. Maximum slit width is defined by the dimensions of the test optic and its radius-of-curvature,  $R_c$ . A maximum width of

$$\delta_{\max} = \frac{R_c \lambda}{4h} \quad (4)$$

where  $h$  is the test piece height,

will result in an intensity distribution which varies less than 20% from the center to the edge of the test optic.

For a 4 in. (10 cm) cylindrical concave mirror with a 260 in. (660 cm) radius-of-curvature, the slit length should be at least 10 cm and the slit width should be no more than  $8 \mu\text{m}$ . To maximize fringe contrast at the viewing screen, the reference beam power must be reduced to approximately that of the object beam; appropriate beam splitter reflectivities are listed in Table 2. All optical elements must be flat to within  $\lambda/56$  to yield  $\lambda/8$  system absolute accuracy, or must be within  $\lambda/21$  for  $\lambda/8$  rms accuracy. Based on this system and assuming a 4 watt laser is used, the light intensity on the viewing screen should be about  $8.5 \times 10^{-7}$  watts/cm<sup>2</sup>, which is sufficient for photographing.

TABLE 2. SLIT INTERFEROMETER COMPONENT REFLECTIVITIES

Splitter No. (see Figure 17)	Reflectivity - %
1	2.2
2	2.2
3	50.0
4	50.0

SECTION IV  
CONCLUSIONS AND RECOMMENDATIONS

1. Cylindrical optical figures deviating from a best fit true surface by  $\lambda/4$  ( $\pm 0.00005$  in.) in 4 in. x 4 in. molybdenum and glass apertures can be considered state-of-the-art.
2. Surface finish and surface quality of  $80 \text{ \AA}$  and 60/40, respectively (scratch and dig as defined by MIL-O-13830A) can be considered feasible.
3. It is impractical (based on cost and time) to quantitatively determine the effects of the several cylindrical polishing process variables because of the large number of interacting variables and because of the lack of control of the variables.
4. Because quantitative effects during spherical polishing are not clearly understood, it was impossible to relate cylindrical polishing to the spherical polishing process.